Dynamics and regulation at the tip : a high resolution view on microtubele assembly

Munteanu, L.

CHAPTER

4

Reconstitution of a microtubule plus-end tracking system *in vitro*

Growing microtubule plus ends have emerged as dynamic regulatory sites in which specialized proteins, called plus-end-tracking proteins (+TIPs), bind and regulate the proper functioning of microtubules [19,20,22,23]. However, the mechanism by which +TIPs regulate microtubule dynamics and the molecular mechanism underlying the +TIP ability to track the growing end are not well understood. An in vitro approach is necessary to understand the effect of individual +TIPs. Here we report the in vitro reconstitution of a minimal plus-end tracking system consisting of the three fission yeast proteins Mal3, Tip1 and the kinesin Tea2. Using time-lapse total internal reflection fluorescence microscopy, we show that the EB1 homologue Mal3 has an enhanced affinity for growing microtubule end structures as opposed to the microtubule lattice. This allows it to track growing microtubule ends autonomously by an end recognition mechanism. In addition, Mal3 acts as a factor that mediates loading of the processive motor Tea2 and its cargo, the CLIP170 homologue Tip1, onto the microtubule lattice. The interaction of all three proteins is required for the selective tracking of growing microtubule plus ends by both Tea2 and Tip1. Our results dissect the collective interactions of the constituents of this plus-end tracking system and show how these interactions lead to the emergence of its dynamic behavior. We expect that such in vitro reconstitutions will also be essential for the mechanistic dissection of other plus-end tracking systems.

Microtubules are polar, dynamic tubulin polymers that have a variety of functions in eukaryotic cells [6]. The dynamics and the spatial organization of microtubules are regulated by several highly conserved microtubule-associated proteins. An important class of these proteins, called +TIPs, accumulates selectively at growing microtubule plus ends in living cells. A wealth of fluorescence microscopy studies in various organisms have identified numerous +TIPs that belong to conserved subfamilies: CLIP-170 [171], APC [172], EB1 [173], CLASPs [174], p150 [175] and spectraplakins [176]. In the fission yeast *Schizosaccharomyces pombe*, classical genetics combined with real-time fluorescence microscopy [177] demonstrated that multiple aspects of cellular organization depend on a defined distribution of microtubules [178, 179]. This distribution is mediated by, among others, three +TIPs: the EB1 homologue Mal3 [109], the

CLIP170 homologue Tip1 [107] and the kinesin Tea2 [41, 180]. A hierarchy of molecular events required for plus-end tracking has been established from observations inside living yeast cells: the motor Tea2 and its putative cargo Tip1 move along the microtubule lattice towards its growing plus ends, where they accumulate [41, 103]. Efficient recruitment to microtubules and the plus-end accumulation of Tea2 and Tip1 depend on the presence of Mal3, which itself tracks the microtubule plus ends independently of Tea2 and Tip1 [41, 103, 109]. It is not yet known whether additional factors or post-translational modifications are required, or whether Mal3, Tea2 and Tip1 constitute a minimal system that is sufficient to show plus-end tracking. In fact, a mechanistic understanding of plus-end tracking is still missing, in part because of the lack of an *in vitro* assay in which plus-end tracking can be reconstituted with a minimal set of pure components [17].

4.1 Results and discussion

Here we reconstitute microtubule plus-end tracking of three fission yeast purified proteins, namely Mal3, Tea2, and Tip1, *in vitro*. The experimental set-up is schematically shown in figure 4.1 a. We observed fluorescently labelled +TIPs and dynamic microtubules by two-color spinning-disc confocal[1] and total internal reflection fluorescence (TIRF)[2] microscopy. Dynamic microtubules were nucleated from short stabilized microtubule seeds attached specifically to a passivated glass surface (see section 4.3).

We first imaged dynamic microtubules in the presence of all three +TIPs: Mal3, Tea2 and green fluorescent protein (GFP)-tagged Tip1 using confocal microscopy. Remarkably, Tip1-GFP was able to accumulate and follow the growing ends of the dynamic microtubules (figure 4.1 b). As Tip1 is at the top of the hierarchy among the three proteins (being the cargo of the kinesin Tea2 and depending on the presence of Mal3 to accumulate at microtubule plus-ends *in vivo*), the three proteins were probably all present at the microtubule tip forming an end-tracking ternary complex. The movie sequence in figure 4.1 b reveals the end-tracking features of Tip1-GFP: i) In the presence of the three +TIPs, Tip1-GFP followed the growing microtubules ends and did not accumulate at the ends of shrinking microtubules or at the static ends of the seeds. ii) Both the plus and the minus ends showed Tip1-GFP accumulation. iii) The intensity of the GFP signal at the microtubule plus end was higher than at the minus end. Also, at the minus end the signal was often blinking during the microtubule elongation, whereas at the plus end the intensity was not visibly fluctuating. The differences in the signal at the two ends indicate that Tip1-GFP in the presence of the three protein complex accumulates preferentially at the microtubule plus-end. The high fluorescence intensity of the tip accumulation indicates the presence of multiple Tip1-GFP molecules following the microtubule end and, most probable, multiple Tea2 and Mal3 molecules.

[1] The confocal microscopy of dynamic microtubules and +TIPs was done at AMOLF.

[2] The TIRF microscopy of dynamic microtubules and +TIPs was done at EMBL.

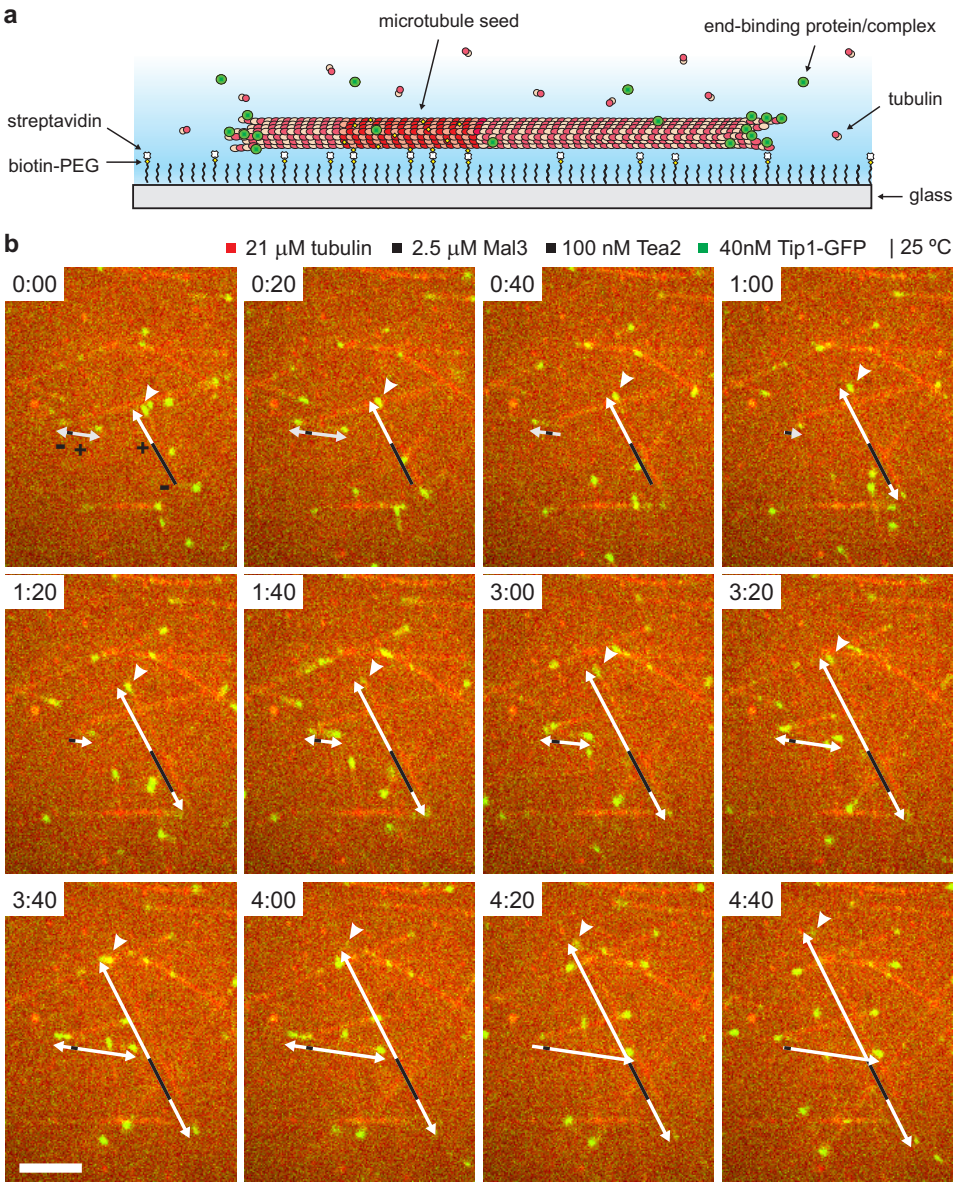

Figure 4.1: Reconstitution of plus-end tracking *in vitro*. **(a)** Diagram of the experimental set-up and **(b)** image sequence showing dynamic microtubules (red) assembled from rhodamine-labelled tubulin in the concomitant presence of Mal3, Tea2 and Tip1-GFP (green). Microtubules were nucleated from surface bound seeds and observed by dual-color spinning-disc confocal microscopy. Schematic guiding lines (shifted with respect to the image) indicate dynamic microtubules (white lines, arrowed if the end is growing) and the corresponding seeds (black lines). Tip1-GFP accumulated and followed only growing microtubule ends, both the plus and the minus end. The intensity of the GFP signal at the plus end (white arrowhead) was higher and less variable during growth as compared with the signal at the minus end. The time elapsed from the first image is indicated in min : sec. Scale bar is 5 µm.

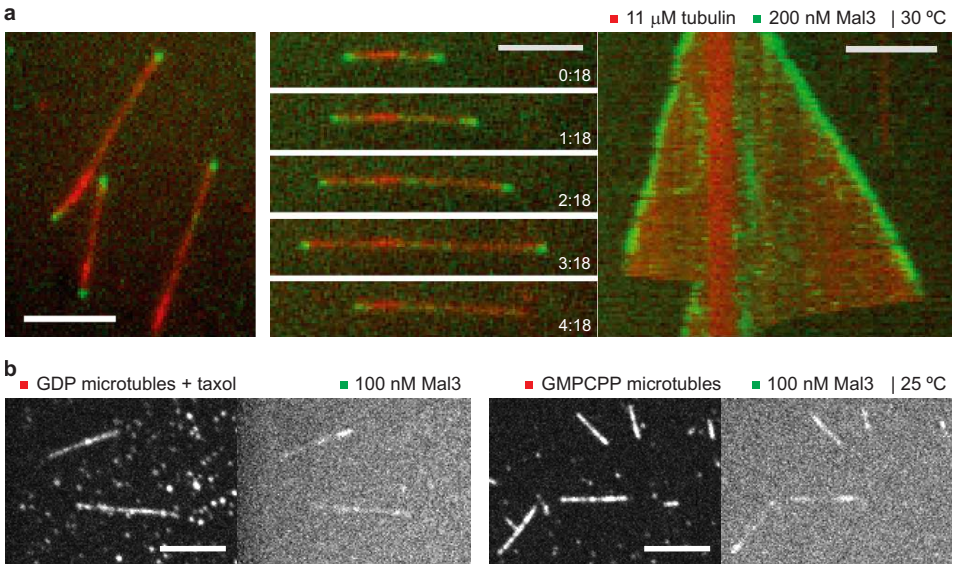

Figure 4.2: Tracking of growing microtubule ends by Mal3 *in vitro*. **(a)** Overlaid TIRF images of Mal3-Alexa 488 (green) and dynamic Alexa 568-labelled microtubules (red). The time sequence of images taken at the indicated times in min : sec (middle) and the corresponding kymograph of the same microtubule (right) shows Mal3 following both growing microtubule ends. Mal3 was used at 200 nM in all end-tracking experiments, unless otherwise stated. The kymograph displays a period of 5 min. Scale bars, 5 μm. **(b)** Confocal images of static microtubules (left image in each pair) in the presence of 100 nM Mal3-Alexa488 (right image in each pair). Mal3 did not accumulate at the ends of static microtubules neither for the taxol-stabilized GDP microtubules (left pair of images) nor for the microtubules assembled with GMPCPP (equivalent with a GTP-tubulin lattice) (right pair). Scale bars, 5 μm.

This first experiment showed that the minimal complex formed by the three proteins is sufficient to reconstitute *in vitro* the microtubule end-tracking by Tip1-GFP. This specific end-tracking behavior seemed to be insensitive to the exact protein concentrations over a wide range of concentrations (lowest combination: 100 nM Mal3, 20 nM Tea2, 8.5 nM Tip1; highest combination: 2.5 μM Mal3, 100 nM Tea2, 45 nM Tip1). We next studied the three +TIPs individually and then in various combinations with fluorescently labelled and unlabelled +TIPs.

4.1.1 Mal3 recognizes and autonomously tracks microtubule growing ends

Only one of the three proteins, the EB1 homologue Mal3, was able to bind efficiently to dynamic microtubules in the absence of the others. Alexa 488-labelled Mal3 selectively accumulated at growing microtubule ends (figure 4.2 a, left) at considerable ionic strength over a wide range of protein concentrations [124]. A Mal3 signal at microtubule tips could be detected even at Mal3 concentrations as low as 7 nM. (see also sec-

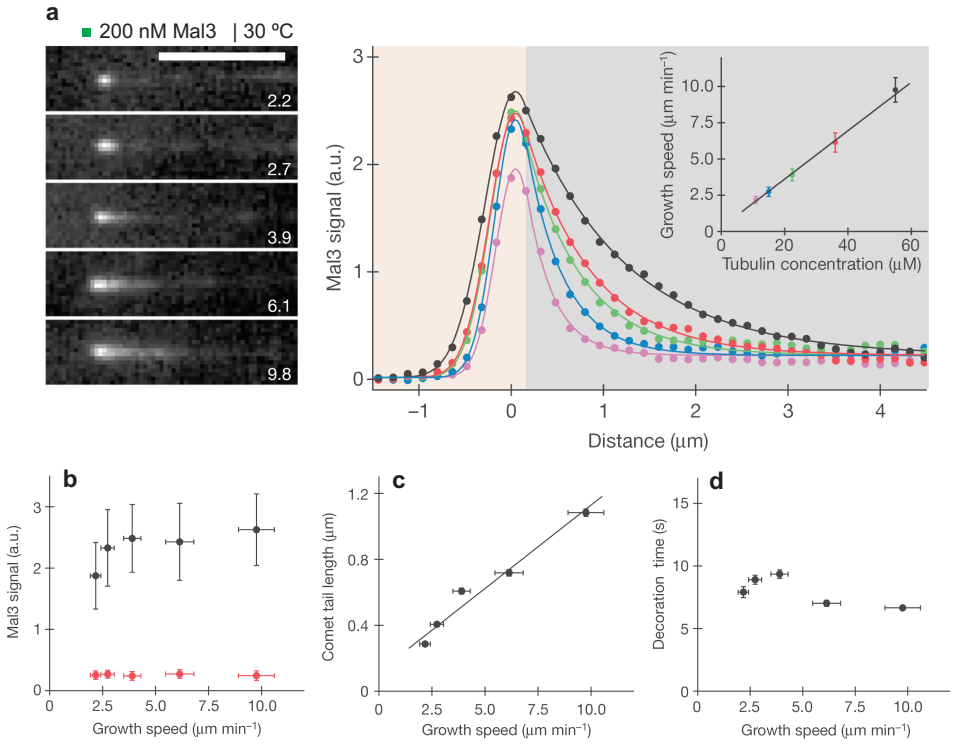

Figure 4.3: Mechanism of plus-end tracking by Mal3. **(a)** Images of individual Mal3-Alexa 488 comets at the indicated growth velocities (in $\mu m\,min^{-1}$) (left) and averaged intensity profiles of the comets (right). The Mal3-Alexa 488 concentration was 200 nM. The data (dots) were fitted (lines) using Gaussian (area to the left from the intensity peak) and exponential (area to the right from the intensity peak) functions. The inset shows the dependence of the growth velocities on tubulin concentrations. Error bars indicate s.d. **(b)** The Mal3-Alexa 488 signal at the peak of the Mal3 comet (black symbols) as obtained from the averaged intensity profiles, and the signal on the microtubule lattice behind the comet (red symbols) as quantified separately from intensity line scans. Error bars indicate the s.d. of the maximum tip intensity and the s.d. of the averaged line scans for the lattice intensity. **(c)** Mal3 comet tail lengths as obtained from single-exponential fits to the averaged intensity profiles. Error bars indicate standard errors as obtained from the exponential fits. **(d)** The characteristic decoration time of the Mal3 signal in the Mal3 comet tail at different microtubule growth speeds as obtained by dividing the comet tail length by the microtubule growth speed. Errors were calculated by error propagation.

tion 5.2.2). Movie sequences and the corresponding kymographs (time-space plots), revealed that Mal3 was tracking both the fast-growing plus ends and the more slowly growing minus ends (figure 4.2 a, middle and right). However, Mal3 did not accumulate at the ends of depolymerizing microtubules (figure 4.2 a, middle and right) or static microtubules (figure 4.2 b). Selective tracking of free, polymerizing microtubule ends is therefore an inherent property of Mal3. Mal3-Alexa 488 also bound weakly along

the entire length of microtubules (figure 4.2 a), a behaviour that was enhanced at lower ionic strength (figure 4.2 b). This binding might reflect the previously shown preferential association of Mal3 with the lattice seam of taxol-stabilized microtubules [25].

Two fundamentally different molecular mechanisms can be envisaged for how Mal3 accumulates at the growing microtubule end. Mal3 could co-polymerize in a complex with tubulin to the growing microtubule end, and subsequently be released. Alternatively, instead of binding to free tubulin, Mal3 could recognize a characteristic structural feature at the microtubule end. This structural feature could either be a collective property of several tubulin subunits such as the previously observed protofilament sheet [34] or a property of individual tubulin dimers that are in a GTP-bound versus a GDP-bound state [99].

We investigated the binding of Mal3 on static microtubules that mimic either GTP-bound or GDP-bound tubulin lattice. The microtubules assembled in the presence of GTP and stabilized by taxol will have predominantly GDP-tubulin within the lattice, whereas the microtubules assembled in the presence of GMPCPP, a slowly hydrolyzable analogue of GTP, are equivalent with a microtubule composed of GTP-tubulin subunits. Mal3 had similar affinity for both type of microtubules (figure 4.2 b), indicating that Mal3 most probably does not recognized the growing microtubule end by preferential binding to GTP-tubulin, which is prevalent at the growing tips.

To distinguish between a co-polymerization mechanism and an end-recognition mechanism, we measured the spatial distribution of Mal3 along microtubule plus ends that were growing in the presence of various tubulin concentrations but a constant Mal3 concentration.

Increased microtubule growth velocities resulting from increased tubulin concentrations led to a more comet-shaped accumulation of Mal3-Alexa 488 at growing microtubule plus ends (figure 4.3 a). Averaged fluorescence intensity profiles of Mal3-Alexa 488 comets demonstrated that after an initial peak in fluorescence the signal decreased exponentially towards the basal lattice signal (figure 4.3 a). The peak fluorescence of Mal3 was largely insensitive to changes in the tubulin/Mal3 ratio (figure 4.3 b). This argues against a simple co-polymerization mechanism, because such a mechanism would lead to peak signals that varied with the tubulin/Mal3 ratio. Furthermore, gel-filtration experiments showed that Mal3 does not bind to unpolymerized tubulin [124]. This agrees with the observation that the amount of Mal3 binding along the microtubule lattice is also independent of the tubulin concentration (figure 4.3 b). Together these data support a mechanism in which Mal3 tracks microtubule ends by recognizing a structural feature.

The characteristic comet tail length obtained from exponential fits to the decays of the averaged Mal3 fluorescence intensity profiles increased linearly with the microtubule growth velocity (figure 4.3 c). This suggests that microtubule ends are decorated with Mal3 for a characteristic time of about 8 s, independently of microtubule growth velocity (figure 4.3 d). In contrast, the dwell time of individual Mal3-Alexa 488 mole-

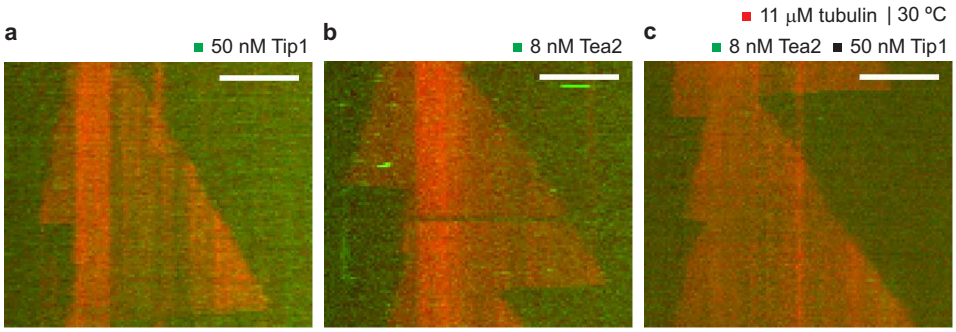

Figure 4.4: Tea2 and Tip1 individually and in combination do not track microtubule ends at physiological conditions. Kymographs of **(a)** Tip1-GFP, **(b)** Tea2-Alexa 488, and **(c)** Tea2-Alexa 488 together with Tip1 (labelled +TIPs in green) on dynamic Alexa 568-labelled microtubules (red). The sensitivity for GFP and Alexa 488 detection was strongly increased in comparison with that in figure 4.2 a. Concentrations were 50 nM for Tip1 and 8 nM for Tea2 in all end-tracking experiments unless otherwise stated. The kymographs display a period of 5 min. Scale bars, 5 μm.

cules at growing microtubule plus ends, measured with greater temporal resolution under single-molecule imaging conditions, was only 0.282 ± 0.003 s [124]. This indicates that individual Mal3 molecules turn over rapidly on a plus-end-specific structure that has a lifetime of about 8 s before it transforms into a normal microtubule lattice structure. A similarly fast turnover of Mal3 was also observed *in vivo* [103].

4.1.2 Tea2 and Tip1 need each other and Mal3 for efficient plus-end tracking

In contrast to Mal3, Tip1-GFP and Alexa 488-labelled Tea2 did not bind significantly to the microtubules in conditions under which selective end tracking of Mal3 was observed (figure 4.4 a and b). Under single-molecule imaging conditions, however, rare interactions of the kinesin Tea2 (0.5 nM) with the microtubule could be observed at low ionic strengths with the use of higher frame rates [124]. The analysis of the motion of single Tea2 motors yielded a mean velocity of 4.8 ± 0.3 μm min^{-1} and an average run length of 0.73 ± 0.01 μm [124]. At the same low ionic strength, but at higher concentration, Tea2 (50 nM) bound efficiently to microtubules (figure 4.5 a and b). A Tea2 profile with continuous increase towards the plus-end and a higher accumulation at the tip was observed on static microtubules. The end accumulation could be due to the motors that land close to the microtubule tip (at a distance from the tip smaller than the average run length) leading to the motors dwelling for a while at the tip before releasing from the microtubule. Intensity profiles along microtubules revealed that more Tea2 motors were present on the taxol-stabilized GDP microtubules (figure 4.5 a) than on the GMPCPP microtubules (figure 4.5 b). It is possible that Tea2 has higher affinity

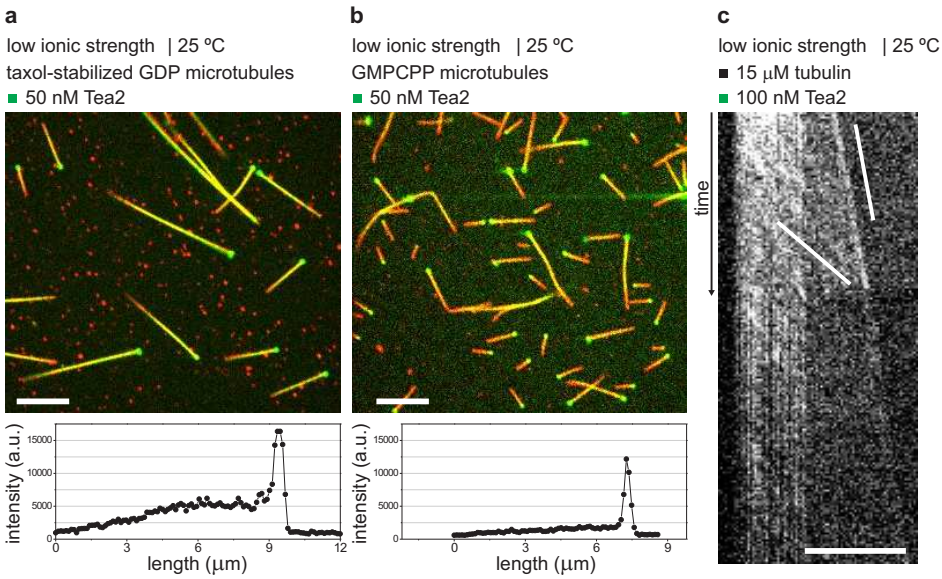

Figure 4.5: Tea2 binds, walks on and end-tracks growing microtubules at low salt conditions. **(a)** and **(b)** Overlaid spinning-disc confocal images of stabilized microtubules (red) and Tea2-Alexa 488 (green). At low salt conditions and in the absence of free tubulin Tea2-Alexa 488 binds efficiently and walks on static microtubules. The kinesin accumulates at the microtubule plus ends. The line intensity profiles along one microtubule shows that more Tea2 was present on **(a)** taxol-stabilized GDP microtubules than on **(b)** the GMPCPP microtubules. **(c)** Kymograph of Tea2-Alexa 488 tracking the plus-end of a dynamic microtubule (same low salt condition as in **(a)** and **(b)**. On the microtubule lattice Tea2-Alexa 488 motors moved towards the plus end with a speed higher than the microtubule growth speed. Two lines are drawn as guidance to the eye: one indicating microtubule growth and one indicating Tea2 speckle movement along the microtubule lattice. The kymograph displays a period of 400 sec. Scale bars, 5 μm.

for the GDP-tubulin lattice and/or the run length of the motor is increased on the GDP-microtubules. Both the single molecule experiments and the binding on the static microtubules were performed in the absence of free tubulin. When we imaged Tea2-Alexa 488 on dynamic microtubules (where free tubulin is present), at low ionic strength conditions, surprisingly, we observed Tea2 tracking the growing plus-ends. The efficiency of binding to the microtubules was though much lower than in the absence of free tubulin. The mechanism of tracking dynamic ends could be understood in a similar way with the accumulation at the microtubule static ends, as the Tea2 kinesin walks faster than the microtubules grow. Using kymograph analysis of the Tea2 motion on dynamic microtubules we measured an average motor speed of 3.5 ± 0.8 μm min^{-1}, which was 6-fold higher than the microtubule growth speed 0.6 ± 0.1 μm min^{-1}. We cannot completely exclude the possibility of Tea2 accumulation at the end due to an unnatural aggregation induced by the low ionic strength. Though, if aggregation of the motor

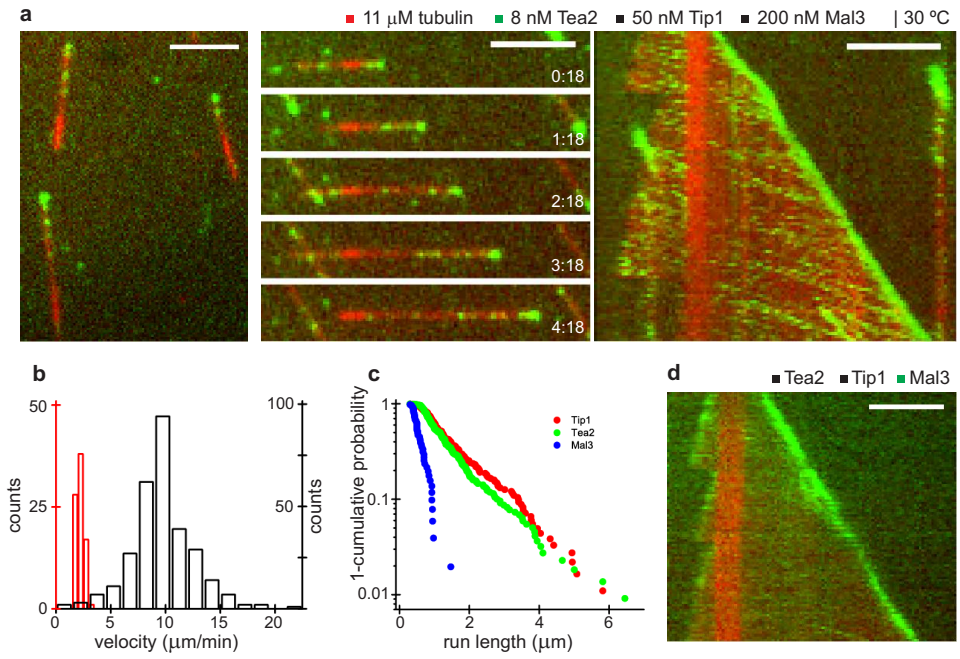

Figure 4.6: Efficient microtubule plus-end tracking of Tea2-Tip1 in the presence of Mal3. (a) Overlaid TIRF images showing Tea2-Alexa 488 (green) and Alexa 568-labelled microtubules (red) in the presence of the two other +TIPs (left). Middle, time sequence of images (at the times shown, in min : sec); right, the corresponding kymograph. Protein concentrations for Mal3 are as in figure 4.2 and for Tea2 and Tip1 as in figure 4.4. Kymographs display periods of 5 min. Scale bars, 5 µm. **(b)** Histograms of the velocities of microtubule plus-end growth (red, left axis) and Tea2-Alexa 488 speckle movement along the microtubule lattice (black, right axis). The increased velocity of Tea2 speckles in comparison with single Tea2 molecules is mostly a consequence of an increased temperature. **(c)** Run-length distribution of Mal3-Alexa 488 (green), Tip1-GFP (black) and Tea2-Alexa 647 (blue) moving along the microtubule lattice, always in the presence of the other two +TIPs. Concentrations were 100 nM Mal3, 50 nM Tip1 and 8 nM Tea2. **(d)** Kymograph showing Mal3-Alexa 488 (green) in the presence of Tea2 and Tip1. The signal intensity can be directly compared with figure 4.2 a.

would predominate, artifacts would appear also on the lattice of static microtubules as local accumulations, which we do not observe in our sample. This experiment suggests that microtubule plus-end tracking is an intrinsic ability of Tea2, but at higher ionic strengths (physiological conditions) Tea2 is not able to efficiently follow growing plus-ends on its own. The preference of Tea2 for the GDP lattice (observed in the absence of free tubulin) could entail that the main role of Tea2 is to assure the efficient transport of other +TIPs to the microtubule tip where these hitchhikers could accumulate and exert a specific function.

Because Tea2 binds *in vivo* [109] and *in vitro* [124] to Tip1, and because the motor might be auto-inhibited without its putative cargo, we tested whether Tip1 could en-

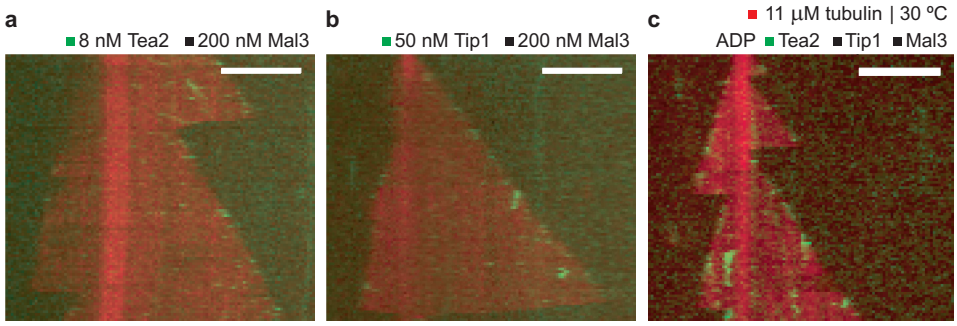

Figure 4.7: All three +TIPs and the motor activity of Tea2 are required for microtubule plus-end tracking of the Tea2-Tip1 complex. (a) Tea2-Alexa 488 (green) in the presence of Mal3 alone does not bind efficiently to microtubules (red). The fluorescence signal can be directly compared with figure 4.4 middle. **(b)** Tip1-GFP (green) in the presence of Mal3 alone does not bind efficiently to microtubules (red). The fluorescence signal can be directly compared with figure 4.4 left. **(c)** The motor activity of Tea2 is required for its microtubule plus-end tracking ability: Tea2-Alexa 488 (green) in the presence of Mal3, Tip1 and ADP instead of ATP. The signal intensity can be directly compared with figure 4.6 a. Standard concentrations of 200 nM Mal3, 50 nM Tip1 and 8 nM Tea2 were used. Kymographs display periods of 5 min. Scale bars, 5 µm.

hance the binding of Tea2-Alexa 488 to dynamic microtubules. However, this was not the case (figure 4.4 c).

In vivo, the presence of Mal3 is needed for the plus-end tracking of Tea2 and Tip1 [41, 103, 109]. Triggered by this observation together with our first successful *in vitro* reconstitution of the end-tracking by the three protein complex we examined whether the autonomous plus-end tracking protein Mal3 is sufficient to mediate microtubule plus-end tracking of Tea2 and Tip1 alone. We investigated in further detail the localization and the end-tracking behavior of the individual +TIPs when all three proteins were present.

At high ionic strengths, in the presence of Mal3 and Tip1, Tea2-Alexa 488 strongly accumulated at growing microtubule plus ends (figure 4.6 a). No accumulation of Tea2-Alexa 488 was visible at growing minus ends (figure 4.6 a) or depolymerizing ends at this condition. Furthermore, Tea2-Alexa 488 speckles appeared along the microtubule lattice and moved towards the plus end (figure 4.6 a, right). The speed of these particles was on average 9.8 ± 2.9 µm min^{-1} and therefore 4.4-fold faster than the velocity of microtubule growth (2.2 ± 0.3 µm min^{-1}; figure 4.6 b). Tip1-GFP moved similarly along the microtubule lattice and also tracked growing microtubule plus ends, but not depolymerizing ends or the ends of static microtubules [124]. Some accumulation at the growing minus ends was though observed at increased concentrations of proteins (see figure 4.1). Mal3-Alexa 488, in contrast, was not observed to move along the microtubule to the same extent as Tea2 and Tip1 (figure 4.6 d). These observations very closely mimic the situation *in vivo* [41, 103, 109].

In addition, Mal3-mediated recruitment of the Tea2-Tip1 complex requires the presence of both Tea2 and Tip1. Tea2-Alexa 488 was hardly present on the microtubules in the absence of Tip1 (figure 4.7 a) and Tip1-GFP was not significantly bound to microtubules in the absence of Tea2 (figure 4.7 b), whereas binding of Mal3-Alexa 488 to microtubules was unaffected in both cases. The results with the double combinations of proteins (figure 4.4 c and figure 4.7 a and b) exactly mimic the *in vivo* single-deletion mutants of Mal3, Tea2 and Tip1 [41, 103, 109].

4.1.3 Mal3 acts as a loading factor for the Tea2-Tip1 complex

Gel filtrations demonstrated that in solution Mal3, Tea2 and Tip1 exist as a stable ternary complex [124]. It is therefore most likely that the formation of this complex is required for efficient binding of Tea2-Tip1 to the microtubule. However, the three proteins do not behave in the same way once bound to the microtubule. Imaging the movements of the three proteins on the microtubule lattice with greater temporal resolution showed that Tip1-GFP and Alexa 647-labelled Tea2 co-migrate [124], indicating that Tea2 indeed transports Tip1. Consistent with this was the observation that the average run lengths for Tea2 and Tip1 were very similar, at 0.90 ± 0.01 and 1.10 ± 0.01 μm, respectively (figure 4.6 c). In contrast, Mal3-Alexa 488 showed only short runs with an average run length of 0.29 ± 0.01 μm (figure 4.6 c). This demonstrates that Mal3 is initially transported by Tea2, but dissociates shortly after a productive binding event.

We confirmed that Mal3-mediated recruitment of Tea2-Tip1 to the microtubule lattice requires the interaction of Mal3 with the amino-terminal extension of the kinesin Tea2 [181]. Replacing full-length Tea2 with a construct lacking the N-terminal extension (ΔNTea2) abolished efficient binding of Tip1-GFP to the microtubule [124].

Replacing ATP with ADP eliminated the efficient binding of Tea2-Alexa 488 along the microtubule lattice and the tracking of microtubule plus ends, despite the presence of all three proteins (figure 4.7 c). Only a very weak fluorescence signal could be observed at growing microtubule ends, but without a preference for the plus or minus end (figure 4.7 c). This demonstrates that *in vitro* the processive motor activity of Tea2 is essential for efficient microtubule-end tracking of Tea2-Tip1 and also for their plus-end preference.

4.1.4 Microtubule dynamics in the presence of Mal3, Tea2 and Tip1

In living cells, single deletions of Mal3, Tea2 or Tip1 suggested that these three +TIPs mainly decrease the frequency of microtubule catastrophes without strongly affecting the other parameters of microtubule dynamic instability [107, 109, 180]. We tested the direct effect of Mal3 alone and of Mal3 with Tea2 and Tip1 on microtubule dynamics under conditions of selective end tracking. We imaged microtubules in the presence of unlabelled +TIPs by differential interference contrast microscopy. At the conditions selected for the end-tracking experiments, neither Mal3 alone nor the combination of

Mal3	Tea2	Tip1	v_{gro} (μm/min) (n)	v_{shr} (μm/min) (n)	T_{cat} (s) (N_{cat})	N_{res} in total time of shrinkage
-	-	-	1.2 ± 0.2 (62)	26 ± 9 (41)	650 ± 80 (69)	0 in 322 s
+	-	-	1.3 ± 0.2 (63)	26 ± 8 (74)	230 ± 20 (132)	8 in 314 s
+	+	+	1.3 ± 0.2 (54)	27 ± 9 (40)	410 ± 50 (61)	4 in 321 s

Table 4.1: Dynamic instability parameters of microtubules in the absence and presence of +TIPs. Dynamic instability parameters under conditions of selective end-tracking (200 nM Mal3, 50 nM Tip1 and 8 nM Tea2). The mean growth velocity (v_{gro}) and mean shrinkage velocity (v_{shr}) represent the weighted averages (weights are the time spanned by each event) over a total of n events. The error on the mean is the weighted standard deviation (s.d.). The average time until a catastrophe occurred (T_{cat}) is the total growth time (summed over individual events) divided by the number of catastrophes observed (N_{cat}). The error on T_{cat} is the standard deviation (s.d.) calculated as $T_{cat}/\sqrt{N_{cat}}$. The number of rescues (N_{res}) in total shrinkage time is given. The time until a rescue occurred and its statistical error could not be determined due to the limited number of events observed.

all three proteins had a strong effect on the growth and shrinkage velocities of microtubule plus ends (table 4.1). However, Mal3 alone increased the frequencies of catastrophes and rescues (table 4.1). In chapter 5 the effect of Mal3 was investigated in more detail revealing that Mal3 has a complex influence on microtubule dynamics, affecting all dynamic instability parameters. The addition of Tea2-Tip1 counteracted the observed effects of Mal3 (table 4.1). Preliminary experiments on the mechanism of regulation of microtubule dynamics by the combination of all three +TIPs are presented in chapter 7 (section 7.2.1). Our results discussed above show that especially the effect of Mal3 on the catastrophe frequency is different from what would be expected from the corresponding deletion *in vivo*. This is not surprising, because several other proteins not studied here are known to affect the catastrophe frequency [182, 183]. By including these other modulators of microtubule dynamics in the future, our *in vitro* system promises also to lead to the identification of the more complex minimal system that reproduces physiological microtubule dynamics.

4.2 Conclusions

Thus, we have identified Mal3 as an autonomous tracking protein of growing microtubule ends *in vitro*. Mal3 most probably recognizes a structural feature at microtubule ends rather than co-polymerizes as a tubulin-Mal3 complex. As *in vivo*, the behavior of Mal3 *in vitro* does not depend significantly on the presence of Tea2 or Tip1. Furthermore, we identified Mal3-Tea2-Tip1 as a minimal system producing plus-end tracking behavior of Tea2 and Tip1 *in vitro*. This suggests that *in vivo* Tea2, Tip1 and Mal3 may also work as a microtubule plus-end tracking system, independently of other +TIPs. However, *in vivo* part of the Mal3 pool might simultaneously function in 'parallel' end-

tracking systems. The role of Mal3 as a loading factor of Tea2-Tip1 involves the initial formation of a ternary complex that promotes productive encounters of Tea2-Tip1 with the microtubule lattice. Tip1 is subsequently transported by the processive motor Tea2, whereas Mal3 rapidly dissociates and is transported for only short distances.

Our in vitro system provides a powerful new tool to test the proposed mechanisms for microtubule end targeting of different +TIPs [17, 29, 110] and to analyse the interplay between plus-end tracking and the dynamic properties of microtubules that are ultimately responsible for the morphogenetic function of the microtubule cytoskeleton.

4.3 Methods

4.3.1 End-tracking assay using TIRF microscopy[3]

Experimental method. Flow chambers consisting of a biotin-PEG-functionalized coverslip (as described in [184]) and a PLL-PEG passivated glass were assembled. To block the residual nonspecific binding sites on the surface, the flow chamber was incubated with 1% Pluronic F-127 and 50 μg/ml κ-casein in assay buffer on ice. Brightly labelled, short GMPCPP microtubules (containing 20% Alexa 568-labelled tubulin and 7.7% biotinylated tubulin) were attached by means of neutravidin to the biotin-PEG functionalized coverslip. With the use of a custom TIRF microscopy system [124], dynamic microtubules and +TIPs either tagged with GFP or labelled with Alexa fluorophores were observed in the presence of 11 μM dimly labelled tubulin (containing 6.7% Alexa 568-labelled tubulin) in assay buffer (80 mM K-PIPES pH 6.8, 85 mM KCl, 4 mM $MgCl_2$, 1 mM GTP, 1 mM EGTA, 10 mM 2-mercaptoethanol and 2 mM MgATP or 5 mM MgADP) containing 0.1% methylcellulose (4,000 cP; Sigma) and an oxygen scavenger system (20 mM glucose, 200 μg/ml glucose-oxidase, 400 μg/ml catalase). In some experiments with Mal3, the tubulin concentration was varied in order to vary the microtubule growth rate (figure 4.3). Unless stated otherwise, the final concentrations of the labelled and unlabelled +TIP proteins were kept constant at 200 nM Mal3, 50 nM Tip1 and 8 nM Tea2. These protein concentrations were chosen after systematic variation of concentrations to allow the easy visualization of both end tracking and transport along microtubules. The temperature was 30 ± 1^{o}C. The experimental conditions for other measurements mentioned here (determination of individual run length and speed of +TIPs on the microtubules, the speed of single Tea2 molecules on static microtubules, and the dwell time of single Mal3 molecules at the microtubule plus-end) are given in [124]. The +TIP proteins were expressed, purified and labelled as described in [124].

Data analysis. The growth trajectories of microtubules and walking tracks of Tea2-Tip1 speckles were analyzed with kymographs in ImageJ (plug-in developed by Arne

[3]The TIRF experimental set-up is located at EMBL.

Seitz). Single-molecule motility was analyzed with kymographs and by automated particle tracking implemented in a custom software environment [124].

Average run lengths of Tea2, Tip1 and Mal3 speckles and their standard error (figure 4.6 c) were obtained from exponential fits to '1-cumulative probability' distributions of the individual travel distances as determined by kymograph analysis from two independent experiments for each protein. The total number of events analyzed was n = 198 for Mal3-Alexa 488, n = 520 for Tea2-Alexa 647, and n = 182 for Tip1-GFP.

To analyze the shape of Mal3 comets (figure 4.3), line profiles of the fluorescence intensity of Mal3-Alexa 488 at growing microtubule plus ends were aligned and averaged. An exponential fit to the tail of the profile was then used to quantify the decay of the signal. Detailed analysis methods are described in [124].

4.3.2 End-tracking assay using confocal microscopy[4]

Experimental method. Flow chambers were assembled between a pre-cleaned glass coverslip and a microscopy slide. The chamber was incubated with 0.2 mg/ml PLL-PEG-biotin (Susos AG, Switzerland) in assay buffer or 2.5 mg/ml biotin-BSA in acetate buffer (21 mM acetic acid, 79 mM $C_2H_3O_2Na$, pH 5.2) and after rinsing, with 1 mg/ml streptavidin in assay buffer. Short GMPCPP microtubules (containing 17% biotin-tubulin and 7% rhodamine-tubulin) were specifically attached to the functionalized surface by biotin-streptavidin links. The flow chamber was passivated by incubation with 1 mg/ml κ-casein. Dynamic microtubules were assembled in the presence of 21 μM tubulin (containing 5% rhodamine-labelled tubulin) and +TIPs in assay buffer (80 mM K-PIPES pH 6.8, 55 mM KCl, 4 mM $MgCl_2$, 1 mM EGTA) supplemented with 1 mM GTP, 0.2 mg/ml κ-casein, 0.2 mg/ml α-casein, and an oxygen scavenger system (50 mM glucose, 400 μg/ml glucose-oxidase, 200 μg/ml catalase, 4 mM DTT). When Tea2 was present in solution, additional 1 mM ATP was added. The final concentrations of +TIPs for the experiment presented in figure 4.1 were 2.5 μM Mal3, 100 nM Tea2 and 40 nM Tip1-GFP. In the experiment with only Tea2 on dynamic microtubules (figure 4.5 c), the ionic strength of the assay buffer was lowered (12 mM K-PIPES pH 6.8, 4 mM $MgCl_2$, 1 mM EGTA), the tubulin concentration was 15 μM and the solution contained 100 nM Tea2. Labelled and unlabelled tubulin was purchased from Cytoskeleton. The sample was sealed with candle wax. During experiments the sample was kept at constant temperature of 25 ± 1°C.

Confocal microscopy. Fluorescently labelled +TIPs and dynamic microtubules were imaged with a confocal spinning disc microscope, comprising a confocal scanner unit (CSU22, Yokogawa Electric Corp) attached to an inverted microscope (DMIRB, Leica) equipped with a 100x/1.3 NA oil immersion lens (PL FLUOTAR, Leica) and a built-in 1.5 x magnification lens. The sample was illuminated using a 488 nm laser (Sapphire 488-30 CHRH, Coherent Inc.) or a 561 nm laser (85-YCA-015, Melles Griot). Images

[4] The spinning-disc confocal set-up is located at AMOLF.

were captured by a cooled EM-CCD camera (C9100, Hamamatsu Photonics) controlled by software from VisiTech International. Images were acquired with a typical 500 ms exposure time. Laser intensity was varied depending on the labelled protein concentration. The temperature was controlled by maintaining the room at 25 ± 1°C.

Data analysis. The growth trajectories of microtubules and walking tracks of Tea2 speckles were analyzed from kymographs in ImageJ (plug-in developed by Arne Seitz). Weighted averages and weighted standard deviation (see section 4.3.4) were calculated for the microtubule growth speed (n = 13) and the speed of Tea2 speckles (n = 65) on microtubules from one experiment with Tea2 alone on dynamic microtubules.

4.3.3 +TIPs on static microtubules analyzed by confocal microscopy

The samples were prepared in a similar way as for the end-tracking assay. The stabilized microtubules were specifically bound to the biotin-PEG functionalized glass surface by biotin-streptavidin links. The GMPCPP microtubules were prepared by incubation of 30 μM tubulin (containing 17% biotin-tubulin and 2% rhodamine-tubulin) with 1 mM GMPCPP (Jena Bioscience, Germany) at 36°C for 50 minutes. The GTP microtubules were prepared from 50 μM tubulin (containing 17% biotin-tubulin and 2% rhodamine-tubulin) and 1 mM GTP by incubation at 36 °C for 50 minutes and additional 10 minutes after 10-fold dilution with 10 μM taxol (Cytoskeleton) warm solution. Mal3 at a concentration of 100 nM was introduced in assay buffer as described for the end-tracking assay. Tea2 was used at a concentration of 50 nM in low ionic strength assay buffer (12 mM K-PIPES pH 6.8, 4 mM $MgCl_2$, 1 mM EGTA) supplemented with 1 mM ATP, 0.3 mg/ml κ-casein, 0.3 mg/ml α-casein, and an oxygen scavenger system. The solutions did not contained free tubulin or GTP. In the experiments with taxol stabilized microtubules 10 μM taxol was maintained in the protein mix. Temperature was 25 ± 1°C. Samples were imaged with the same confocal spinning disc microscope as above. Line intensity profiles along microtubules were measured in ImageJ.

4.3.4 DIC assay to measure microtubule dynamics

Experimental method. Samples were prepared in a similar way as for the TIRF end-tracking assay. The functionalized surface was created with 0.2 mg/ml PLL-PEG-biotin and 1 mg/ml streptavidin and passivation was done with 0.5 mg/ml κ-casein. The nucleating seeds contained 15% biotin-labelled tubulin only. Protein concentrations were as for the TIRF end-tracking assay. Samples were maintained at 30 ± 1°C.

DIC microscopy. Dynamic microtubules nucleated from surface bound seeds were imaged by video-enhanced differential interference contrast (VE-DIC) microscopy using an inverted microscope (DMIRB, Leica) equipped with a 100x/1.3 NA oil immersion objective (HCX PL FLUOTAR, Leica). The temperature in the sample was adjusted and maintained constant by Peltier elements (Melcor) mounted on a sleeve around the objective and controlled by in-house built electronics. Images were acquired with a CCD

camera (CF8/1, Kappa), further processed for background substraction and contrast enhancement with an image processor (C5510 Argus 20, Hamamatsu Photonics) and digitized on-line at a rate of 1 frame per 2 seconds with an in-house developed software (written and run in IDL). Simultaneously with the on-line digitization, the processed images were recorded on a DVD at video rate with a commercial burner (DVD R-80, Philips).

Data analysis. For the analysis of microtubule dynamics, for every condition DIC data was collected from three independent experiments and for every experiment a minimum of 10 microtubules were analyzed with kymographs. The average growth and shrinkage speeds (table 4.1) were calculated as weighted averages over all events as $v = (\sum_1^n v_i t_i)/(\sum_1^n t_i)$. Individual speeds ($v_i$) were estimated from manual fits to the growth or shrinkage parts of the kymograph. The weights are represented by the times (t_i) spanned by the individual events (i). The error was calculated as weighted standard deviation, derived from $sd^2 = \frac{n}{n-1}(\sum_1^n (v_i - v)^2 t_i)/(\sum_1^n t_i)$. The catastrophe time ($T_{cat}$) was calculated as the total growth time divided by the number of catastrophes observed (N_{cat}) and the statustical error on T_{cat} as $T_{cat}/\sqrt{N_{cat}}$. The number of rescues observed (N_{res}) in total shrinkage time are mentioned (table 4.1).

Acknowledgments

The major part of the experimental work presented in this chapter is published in [124] and was the result of a collaborative effort between AMOLF: Liedewij Laan, myself and Marileen Dogterom and EMBL: Peter Bieling, Henry T. Schek, Linda Sandblad, Thomas Surrey and Damian Brunner.

[124]: Bieling P, Laan L, Schek HT III, Munteanu EL, Sandblad L, Dogterom M, Brunner D, Surrey T (2007) Reconstitution of a microtubule plus-end tracking system *in vitro*. *Nature* **450**: 1100-1105